Photodissociation of Dimethyl Sulfoxide at 193 nm in the Gas Phase

Xirong Chen, Hongxin Wang, and Brad R. Weiner*

Department of Chemistry and Chemical Physics Program, University of Puerto Rico, Box 23346 UPR Station, Río Piedras, Puerto Rico 00931

Michael Hawley† and H. H. Nelson

Chemistry Division, Code 6110, Naval Research Laboratory, Washington, D.C. 20375

Received: June 22, 1993; In Final Form: August 17, 1993®

The photodissociation dynamics of the reaction $(CH_3)_2SO + h\nu(193\ nm) \rightarrow 2CH_3 + SO$ have been examined by laser spectroscopic techniques. Relative vibrational and rotational state energy distributions of the nascent SO photofragment have been determined by using laser induced fluorescence spectroscopy on the $(B^2\Sigma^- - X^3\Sigma^-)$ transition. The same technique has also been employed to establish the quantum yield, $\Phi_{193}[SO(X^3\Sigma)] = 1.02 \pm 0.12$. The nascent vibrational state distributions in the ν_1 and ν_2 modes of the methyl radical have been determined by using 2 + 1 resonance enhanced multiphoton ionization spectroscopy via the $(3p\ ^2A_2'' \leftarrow 2p\ ^2A_2'')$ transition.

Introduction

Understanding the detailed photodissociation dynamics of polyatomic molecules containing more than five or six atoms remains a complicated problem. This complexity arises from the possibility of multiple product channels and the large number of degrees of freedom available for energy partitioning. The measurement of the internal state distributions of the photofragments produced by laser induced fragmentation of polyatomic molecular species can be useful in elucidating the detailed mechanism of the photodissociation process itself.[1] In order to understand the photodissociation of polyatomic molecules at a detailed microscopic level, it is often necessary to evaluate the energy content of more than one of the primary products.[1] For the case of larger molecules, where more than two fragments are produced, the concertedness and/or synchronicity of the multiple bond breaking needs to be addressed.[2]

Dimethyl sulfoxide (DMSO), a widely used solvent, presents an interesting test case on several different levels. As the simplest sulfoxide, DMSO can serve as a model photochemical system. As the sulfur analog of ketones, the unimolecular chemistry of alkyl sulfoxides may provide insight into the molecular orbital bonding picture.[3] $(CH_3)_2SO$ has been postulated as a possible intermediate in the atmospheric sulfur cycle, *i.e.*, in the oxidation of reduced alkyl sulfides to sulfur dioxide.[4] In the laboratory, DMSO has been utilized routinely as a thermal source of methyl radicals[5] and can now be used to photolytically produce the SO radical,[6] an important member of the isovalent series that includes O_2 and S_2.

Photochemical studies of dimethyl sulfoxide in the ultraviolet are limited. Gollnick and Stracke[7] reported indirect evidence for

$$(CH_3)_2SO + h\nu \rightarrow CH_3SO + CH_3 \qquad (1)$$

as the primary process for DMSO photolysis at 254 nm in solution. Chen *et al.* favored this mechanism as the primary step leading to the gas-phase photoproduction of SO at 193 nm but could not prove it conclusively.[6] The alternative mechanism,

$$(CH_3)_2SO + h\nu \rightarrow SO + 2CH_3 \qquad (2)$$

where the parent sulfoxide undergoes simultaneous three-body fragmentation is also a possibility, but the three-center molecular elimination to produce ethane and sulfur monoxide in concert has been ruled out previously.[6]

As stated above, DMSO is the sulfur analog of acetone, $(CH_3)_2CO$. The 193-nm absorption band of acetone has been well-studied, because $(CH_3)_2CO$ provides a model system for a polyatomic molecule which produces three fragments on photodissociation. The direct measurement of the absorption spectrum of acetone suggests that the dissociation occurs by excitation first to a molecular Rydberg state, which is then followed by rapid internal conversion and dissociation into two methyl radicals and a CO molecule.[8] The nascent fragment quantum state distributions have been well-studied in this case. The internal vibrational and rotational state energy distributions, along with the translational energy release into the photoproducts have been experimentally measured for both the methyl and CO fragments.[9] The most recent experimental data and the complimentary information-theoretic analysis suggest that the dissociation occurs by a mechanism, which is in between stepwise and concerted.[2,9d] This cooperation between experiment and theory interprets the dissociation for this model species as occurring by a two-step process, where the initially formed acetyl intermediate has a lifetime comparable to its corresponding rotational period.

The internal and translational energy distributions of nascent SO fragments produced by the photodissociation of SO_2[6,10] and Cl_2SO[6,11-14] have been the subject of several experimental investigations. In a recent letter, Chen *et al.* reported nascent vibrational distributions for the 193-nm photodissociation of SO_2, $SOCl_2$, and $(CH_3)_2SO$ by using the $SO(A^3\Pi - X^3\Sigma^-)$ transition to probe the diatomic photoproduct.[6] In this work, we use the $SO(B^3\Sigma^- - X^3\Sigma^-)$ transition to probe the nascent photofragment following the 193-nm photolysis of DMSO, because it allows us to probe higher ground-state vibrational levels due to the relatively large Franck-Condon factors,[15] and because the rotational structure is much less congested than in the A-X transition. This allows the accurate measurement of nascent rotational-state distributions. From the data obtained here, the relative vibrational- and rotational-state population distributions and the quantum yield of the nascent $SO(X^3\Sigma^-)$ state are measured as well as an upper limit for the kinetic energy imparted to the SO photofragment during the photodissociation process. Furthermore, we have used REMPI spectroscopy to probe the internal energy of the methyl fragments produced by this photodissociation. Previously, REMPI has been used to detect the vibrational-state distribution of methyl fragments from photodissociation of other

* Author to whom correspondence should be addressed.
† NRC/NRL Postdoctoral Research Associate.
® Abstract published in *Advance ACS Abstracts*, October 1, 1993.

0022-3654/93/2097-12269$04.00/0

species, including acetone.[9c,16] This spectroscopic method provides the nascent state population distribution for a few vibrational modes directly. An estimate of the rotational energy content of the methyl fragments produced from the dissociation of DMSO has also been obtained by band contour analysis. By measuring the rovibrational energy content of the three fragments, it will be shown that a more detailed picture of the photodissociation dynamics of DMSO at 193 nm, than that previously described, can now be unraveled.

Experimental Section

Two different experimental apparati were used in this study: (i) an excimer laser photolysis/LIF system at the University of Puerto Rico (UPR) and (ii) an excimer laser photolysis/REMPI experiment with mass-resolved deection at the Naval Research Laboratory (NRL).

UPR Experiments. The LIF apparatus used to measure the nascent energy of the sulfur monoxide photoproduct has been described previously.[6,17] In brief, DMSO, either neat or in a buffer gas, is flowed through a stainless steel reaction chamber, equipped with scattered light reducing extension arms and fused silica windows. DMSO partial pressures (10–200 mTorr) are limited by the room temperature vapor pressure of the compound. All pressures are measured by a capacitance manometer at the cell exit.

The two laser beams, photolysis and probe, are collinearly counterpropagated along the entire length of the cell to ensure maximum overlap in the center of the reaction chamber. Dimethyl sulfoxide is photolyzed at 193 nm by an excimer laser (Lambda Physik LPX205i) operating on the ArF transition. Nascent SO photofragments are monitored by LIF on the ($B^3\Sigma^-$–$X^3\Sigma^-$) transitions in the 237–295-nm region of the spectrum. The probe laser light in this region was generated by frequency doubling (β-BaB_2O_4 crystal) the output of a Lambda Physik FL3002 tunable dye laser (bandwidth = 0.25 cm^{-1}), which is pumped by a Lambda Physik LPX205i excimer laser at 308 nm. To cover the entire frequency range of the SO B-X signal, three laser dyes, Coumarin 480, 503, and 540 A (Exciton, Inc.) were used. The LIF signal was found to be linear over a range of photolysis laser fluences (10–50 mJ/cm^2), indicating that the production of SO occurs by single photon absorption.

Fluorescence is viewed at 90° relative to the laser beam axis by a high gain photomultiplier tube (PMT) through a long-pass filter (Schott WG295). The output of the PMT is processed and averaged by a gated integator (SRS Model SR250), digitized (SRS Model 245), and sent to a microcomputer for display, storage, and analysis. The delay time between the two lasers was controlled with a digital delay pulse generator (SRS Model DG535). For a fixed delay time between photolysis and probe laser, the frequency-doubled output of the dye laser was scanned while collecting the total fluorescence signal to obtain a nascent excitation spectrum. Data were typically collected at 40 Hz.

$(CH_3)_2SO$ (MCB Reagents, 99.9%) was subjected to three freeze–pump–thaw cycles prior to use. Sulfur dioxide (Air Products, 99.8%) was used directly as supplied as a calibrant and an actinometer in the quantum yield experiments.

NRL Experiments. The data for these experiments were obtained in a supersonic free jet, time of flight mass spectrometer (TOFMS), equipped for photoionization. The parent molecule, DMSO, is expanded in a buffer gas of helium through a flat, free-jet nozzle (0.05-cm diameter, General Valve). Total backing pressures were between 100 and 600 Torr, and the expansions were between 0.2 and 1% in DMSO. These low backing pressures were chosen to prevent the formation of clusters in the free jet. No systematic correlation of the experimentally measured methyl spectrum as a function of backing pressure was observed, leading us to conclude that clusters are not contributing significantly to our detailed signals. The gas mixture was allowed to expand

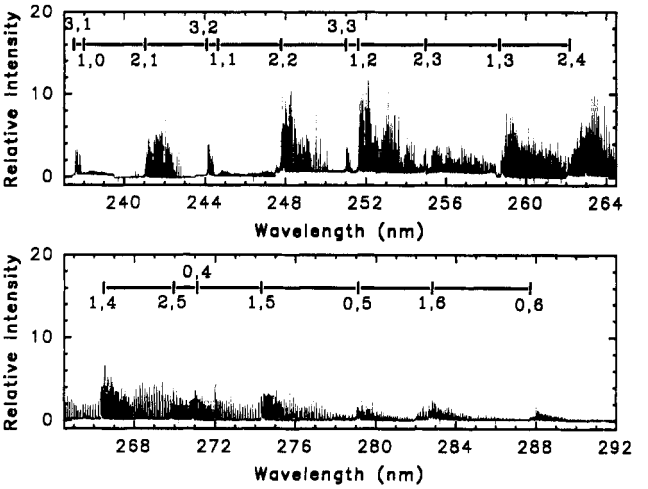

Figure 1. LIF spectrum of nascent SO($X^3\Sigma^-$) from the 193-nm photodissociation of 0.026 Torr of $(CH_3)_2SO$. The delay between the pump and the probe laser was 400 ns. The origins of the vibrational bands have been assigned from ref 19.

unskimmed between the two extraction plates (spacing = 4 cm) of the TOFMS into a chamber pumped by a 10″ diffusion pump. The entrance aperture of the mass spectrometer lies 5 cm below the nozzle at right angles to both the free jet axis and the laser axis. At the point where the mass spectrometer and jet axes intersect, rotational cooling of the precursor has effectively ceased, and an excimer laser (Lambda Physik EMG 101) operating on the 193 nm ArF transition (30 mJ/cm^2) intersects the expanding free jet and photolyzes the DMSO precursor molecules. A second probe laser, delayed by 400 ns with respect to the first, detects the methyl photofragments by REMPI spectroscopy before they can be collisionally relaxed. The transition used is the well-known 2 + 1 ($3p\ ^2A_2'' \leftarrow 2p\ ^2A_2''$) REMPI transition.[5] The probe laser is a frequency-doubled Nd:YAG pumped dye laser (Quantel 581/DL) operating on DCM dye. The output from this laser in the UV is maintained at *ca.* 0.5 mJ per pulse to avoid broadening of the CH_3 REMPI transitions. The probe laser is focused with a 15-cm focal length lens and counterpropagates with the photolysis laser.

The mass spectrometer is of the standard Wiley–McLaren design.[18] In our specific case, the two stage extraction field is followed by two sets of parallel deflector plates. The first set of plates remove the initial jet velocity the ions possess, while the second set defects them onto the ion detector which is a 1″ diameter multichannel plate at the end of a 1.4-m drift tube. The mass spectrum can be observed on a 125-MHz transient digitizing oscilloscope (Lecroy 9400), and REMPI spectra are recorded by sequentially stepping the laser wavelength while averaging the signal in a boxcar integrator (Stanford Research SR250) which is gated for the arrival time of $m/e = 15$. The entire experiment is synchronized by a computer which steps the laser wavelength and collects the data.

Results

1. Internal Energy Distribution of SO($X^3\Sigma^-$). *a. Vibrational-State Distribution.* Under collision-free conditions (DMSO: 0.02–0.03 Torr; probe laser delay = 400 ns), the relative vibrational population of the nascent electronic ground state SO ($X^3\Sigma^-$) from the DMSO photodissociation at 193 nm has been determined by using LIF excitation spectra of SO($B^3\Sigma^-$–$X^3\Sigma^-$) transitions in the region of 237–295 nm (see Figure 1). The bandheads of this electronic transition have been assigned by using the spectroscopic constants reported by Colin.[19] In order to obtain the relative vibrational population of SO ($X^3\Sigma^-$, $v'' = 0$–6), the integrated areas under the (1,0), (1,1), (1,2), (1,3), (1,4), (1,5), and (1,6) vibrational bands are measured and subsequently normalized for

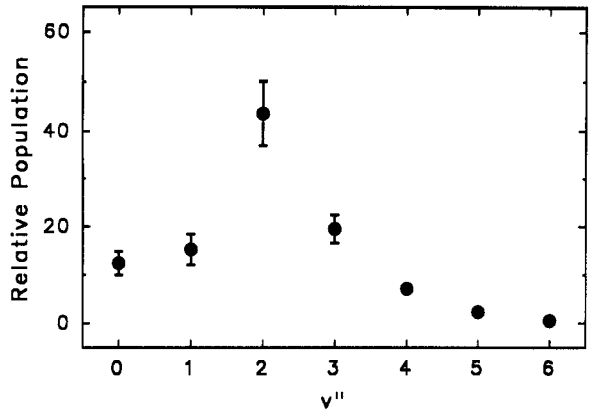

Figure 2. Nascent vibrational state distribution of $SO(X^3\Sigma^-, v')$ from the 193 nm photodissociation of $(CH_3)_2SO$.

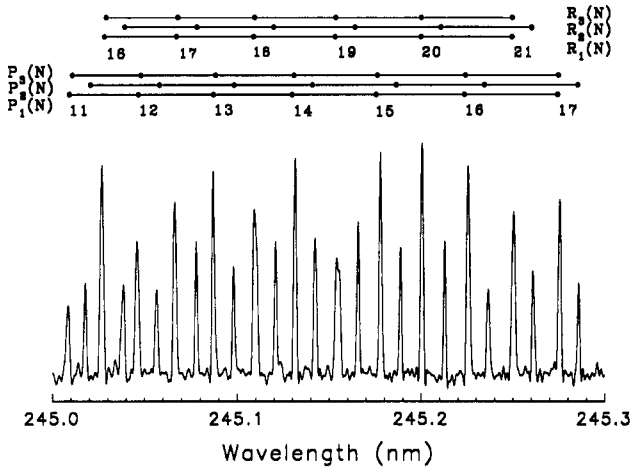

Figure 3. A portion of the $(B^3\Sigma^-, v' = 1 \leftarrow X^3\Sigma^-, v' = 1)$ transition showing the partial assignment of the rotationally-resolved LIF excitation spectrum used for measurement of the rotational population state distribution.

their respective Franck-Condon factors.[15] The nascent vibrational population distribution is shown in Figure 2. The observed vibrational distribution is inverted and peaked at $v'' = 2$, in agreement with previous measurements.[6] The increased sensitivity at higher vibrational levels, now attainable with the B–X transition, can be seen when compared to the previous measurement.[6] No signal for the (1,7) band was detected, even though we have observed it for other photofragmentation cases.[14]

b. Rotational-State Distribution. The rovibronic transitions of SO ($B^3\Sigma^-$–$X^3\Sigma^-$) have been used for the measurements of the rotational-state population distribution. The rotational levels of each of the $^3\Sigma^-$ electronic states are split into three spin components, F_1 for $J = N + 1$, F_2 for $J = N$, and F_2 for $J = N - 1$, primarily by the second-order spin-orbit interaction. There is no Q branch in the $^3\Sigma^-$–$^3\Sigma^-$ transition due to the selection rule: $\Delta N = 0$ is forbidden.[20] Moreover, only $\Delta J = 0$ (*i.e.*, F'_1–F''_1, F'_2–F''_2, F'_3–F''_3) transitions have significant intensity for $N > 10$, because the Hönl–London factors for $\Delta J \neq 0$ transitions decrease rapidly with increasing N.

A portion of the rotationally resolved LIF excitation spectrum of SO ($B^3\Sigma^-, v' = 1$–$X^3\Sigma^-, v'' = 1$) transition is shown in Figure 3. The assignment of the spectrum is based on the calculated line positions using Colin's spectroscopic constants.[19] The difference between the calculated line positions and our experimental measurements are ≤0.005 nm.

The relative rotational-state populations within a given vibrational band, $P(N'')$, can be determined by normalizing the intensity of the transition by the Hönl–London factor and the rotational degeneracy. The integrated area of a given spectral peak is used as the measure of the intensity in these experiments. Hönl–London factors for $^3\Sigma$–$^3\Sigma$ transitions were taken from Smith and Liszt.[15]

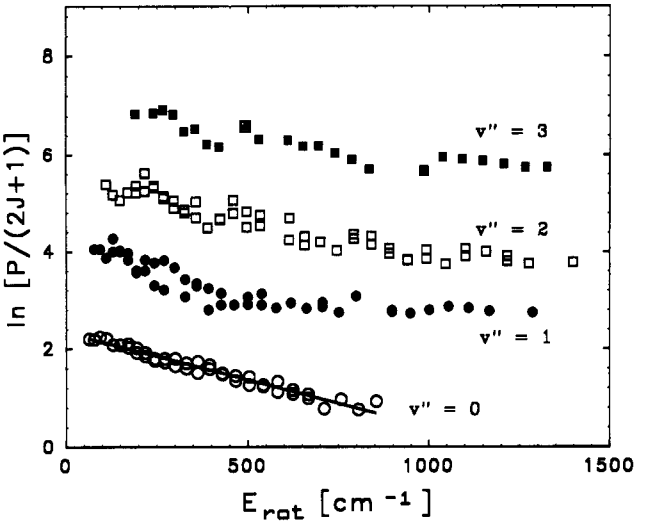

Figure 4. Semilog plot of the intensity of $SO(X^3\Sigma^-, v'')$ rotational lines corrected for the Honl–London factors, measured 400 ns following the 193-nm photolysis of $(CH_3)_2SO$. The solid line is a linear least squares fit to the $SO(X^3\Sigma^-, v'' = 0)$ data and corresponds to a Boltzmann temperature of 748 ● 24 K.

A rotational distribution in a single vibrational level can, in many cases, be described by the Boltzmann expression

$$P(N'') = (2J'' + 1) \exp[-BN''(N'' + 1)/kT_R] \quad (3)$$

where B is the rotational constant of the ground state, k is the Boltzmann constant, and T_R is the rotational temperature. A plot of $\ln[P(N'')/2J'' + 1)]$ vs $BN''(N'' + 1)$ will give a straight line with slope, $-1/kT_R$, and the least-square fits of these points to this form will yield the rotational temperature T_R. Figure 4 is a Boltzmann plot of the nascent rotational-state populations of $SO(X^3\Sigma^-, v'' = 0, 1, 2,$ and 3) that results from DMSO photodissociation at 193 nm. We emphasize that our Boltzmann plots are not rigorously linear (i.e., they cannot be characterized as rotational temperatures) and that linear least squares fits to the data points yield rotational temperatures that are only approximations of the rotational distributions. We present the data in this form only because it serves a useful purpose in comparison of this work with other related studies (see below). The rotational-state populations of $v'' = 0$–3 can be fit by a straight line with rotational temperatures, T_R, in the range of 750–1450 K. In the case of $v'' = 1$, the nascent rotational-state distribution is not as well-represented by a single line as in the other cases.

2. Quantum Yield Determination. Since more than one electronic state of SO is thermochemically accessible in the 193-nm photodissociation of DMSO, we have measured the primary quantum yield of $SO(X^3\Sigma^-)$ following excimer laser photolysis. In our experiments, the LIF signal of a given rotational line of $SO(X^3\Sigma^-, v'' = 2)$ has been used to make this measurement. As mentioned above, the LIF signal intensity of $SO(X^3\Sigma^-)$ was found to be linear with respect to the 193-nm photolysis laser fluence in our experiment indicating that the production of SO radical results from a single photon absorption by the parent molecule. To measure the photofragment quantum yield of $SO(X^3\Sigma^-)$, we compare the LIF signal intensity of a single SO rotational line following the 193-nm photolysis of both DMSO and SO_2. For example, the dye laser is fixed at 252.105 nm corresponding to the $R_{22}(20)$ line of $SO(B^3\Sigma^-, v' = 1 \leftarrow X^3\Sigma^-, v'' = 2)$ transition. Either DMSO or SO_2 (0.02 Torr) is introduced into the reaction chamber, and the LIF signal intensity is averaged for 2000 laser shots. We repeat the experiment ten times and take the average for the quantum yield measurement. Assuming that the

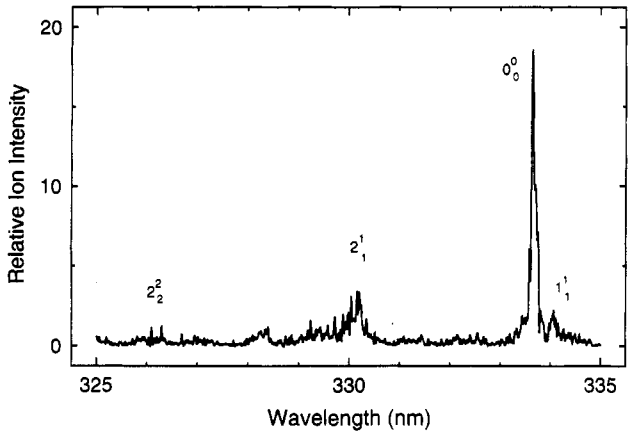

Figure 5. 2 + 1 ($3p^2A_2'' \leftarrow 2p^2A_2''$) REMPI spectrum of CH_3 radicals produced from the 193-nm photodissociation of $(CH_3)_2SO$ obtained by monitoring mass 15. This spectrum has not been normalized for laser power.

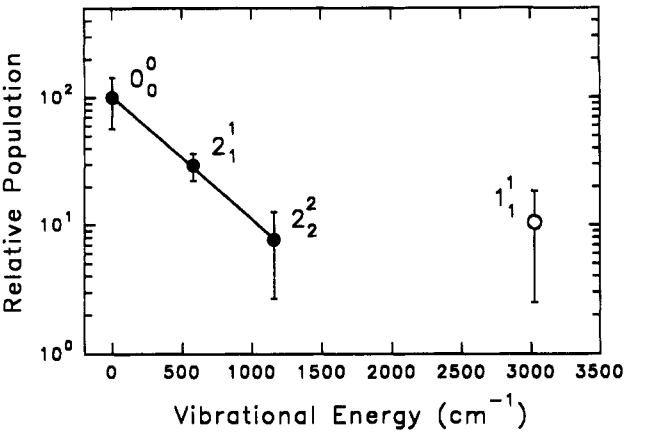

Figure 6. Relative vibrational state distribution for the observed vibrational modes of methyl radical produced from the 193-nm photodissociation of $(CH_3)_2SO$. The line is a Boltzmann fit to the v_2 mode, which results in a vibrational temperature of 600 K.

$SO(X^3\Sigma^-)$ produced by SO_2 photodissociation at 193 nm occurs with unit efficiency, the quantum yield of sulfur monoxide radical production from DMSO photodissociation at 193 nm is found to be $\Phi_{193}^{DMSO}[SO(X^3\Sigma)] = 1.02 \pm 0.12$. The measurement was also repeated for several different rotational lines in the $v'' = 2$ manifold, yielding a similar result. In order to obtain these values, the experimentally obtained signal intensity was corrected for the measured nascent SO photofragment vibration-state distributions resulting from 193-nm photolysis of SO_2 and DMSO and for their absorption cross sections.[21] The nascent $SO(X^3\Sigma, v'' = 2)$ rotational-state distributions for DMSO and SO_2 are similar.[22] A quantum yield measurement was made for longer delay times, *i.e.*, to allow rotational relaxation and relaxation of higher electronic states of SO, and a similar result, 0.91 ± 0.09, was obtained. We have also made quantum yield measurements of the production of $SO(X^3\Sigma^-)$ from the 193-nm photolysis of $SOCl_2$.[14] We obtain a value of $\Phi_{193}^{SOCl_2}[SO(X^3\Sigma)] = 0.73 \pm 0.10$, in strong agreement with the previous measurement of 0.80 by Kanamori *et al.* using infrared absorption spectroscopy.[14]

3. Kinetic Energy of the SO Fragment. Typical line widths (FWHM) of SO rotational lines measured in our experiments are 0.25–0.3 cm^{-1} and are therefore laser limited (0.25 cm^{-1}). This line width can be used as the maximum value of the Doppler profile of SO rovibronic transitions, assuming the DMSO photodissociation to be isotropic, and the translational temperature, T_{trans}, of nascent of $SO(X, v'')$ fragment can be estimated by the following relationship:

$$T_{trans} = (\Delta v/2v_0)^2 mc^2/2k \ln 2 \qquad (4)$$

where Δv is the FWHM of the Doppler profile, v_0 is the center frequency of the given line, m is the molecular mass, and k is the Boltzmann constant. The translational temperature of nascent $SO(X, v'' = 1)$ is found to be <3500 ± 500 K by this estimate, yielding an upper limit for the average translational energy <8.8 ± 1.4 kcal/mol.

4. CH_3 Internal Energy Distribution. A representative REMPI spectrum of the nascent methyl radicals, uncorrected for laser power, is shown in Figure 5. The $m/e = 15$ ion signal arising from the photoionization of methyl is directly proportional to the intensity of the excimer (pump) laser and depends quadratically on the intensity of the doubled dye (probe) laser as would be expected for a 2 + 1 REMPI process. We observe four vibrational bands in the spectrum, 0_0^0, 1_1^1, 1_1^1, and 2_2^2, as designated in Figure 5. Excitation is only observed in the v_2 (umbrella) mode and the symmetric C–H stretch v_1. This result is consistent with the previous product state distributions of photolytic methyl fragments from acetone,[8] methyl iodide,[14] and nitromethane[15] obtained by REMPI.

Figure 6 shows a plot of the observed vibrational population distribution for the methyl radicals produced from the 193-nm photolysis of $(CH_3)_2SO$. Relative populations are determined by integrating under the vibrational band and then correcting for both the laser intensity and the vibrational Franck–Condon factors.[15] As has been pointed out previously, there are difficulties in assigning relative populations from intensities of REMPI transitions.[15] We have used the same approximations as Trentleman et al. in their analysis of acetone.[9c] Following this standard and fitting the population of the observed levels in the v_2 mode to a Boltzmann model produces a vibrational temperature of 600 K. A rotational contour analysis[9,15] of the 0_0^0 band leads to an estimate of the rotational temperature of methyl in the origin band of 150 K. As in the case of acetone, there may be vibrational modes populated which we cannot clearly observe; however, we believe that the relative distribution of the vibrational modes which we do observe is correct.

Discussion

The quantum yield measurement, demonstrating the production of ground-state sulfur monoxide with unit efficiency, limits the number of possible photoreactions to

$$\text{DMSO} + h\nu(193\text{ nm}) \rightarrow SO(X^3\Sigma^-) + 2CH_3$$
$$\Delta H_{RXN} = 106.3 \text{ kcal/mol} \qquad (5)$$
$$E_{avail} = 41.7 \text{ kcal/mol}$$

$$\rightarrow SO(X^3\Sigma^-) + C_2H_6$$
$$\Delta H_{RXN} = 24.8 \text{ kcal/mol} \qquad (6)$$
$$E_{avail} = 123.2 \text{ kcal/mol}$$

While we have not directly measured the photochemical quantum yield of CH_3 radicals in this experiment, we assume (5) to be the only reaction pathway. This assumption is based on (1) the inability to detect ethane in previous experiments[6] and (2) the energy content of the photofragments (see below).

The total energy balance in these experiments is summarized in Table I, assuming that only reaction 5 is operative. Since we can only account for at most 52% of the available energy in the nascent photofragments, we must ask, where is the remaining energy? One possibility is that we have not accounted for all the internal energy in the CH_3 photofragments. Recently, experimental studies have shown that other vibrational states may also be populated which are not observed in our REMPI experiment. Donaldson and Leone, in infrared emission experiments have shown that the v_3 mode of methyl is populated in the photodis-

TABLE I: Distribution of Available Energy into the Different Degrees of Freedom of the Nascent Photofragments Following 193-nm Photodissociation of Dimethyl Sulfoxide

fragment	mode	energy (kcal/mol)	% available energy
CH_3	translational	not measd	
	internal	1.9	4.7
SO	translational	8.8[a]	21.1[a]
	internal	8.9	21.3
CH_3	translational	not measd	
	internal	1.9	4.7

[a] Upper limit.

sociation of acetone.[6] No population is observed in the v_3 mode in the REMPI spectrum of the methyl radical following 193-nm irradiation of $(CH_3)_2CO$ however.[8] Direct time-resolved infrared diode laser absorption spectroscopy experiments on dissociated acetone-d_6 show a rise in the ground vibrational state CD_3 population with a time constant suggesting that many vibrational states may initially be populated,[9] again conflicting with the results of the REMPI study which suggests that most of the molecules are formed in the vibrational ground state. Despite this large discrepancy, the relative populations of the methyl rotational and vibrational states which are observed in both the REMPI and diode laser experiments agree. These important facts underscore the caution that must be exercised when one uses REMPI on a polyatomic molecule to measure state distributions. The REMPI spectrum provides incomplete information (which as an infrared spectrum does) on the vibrational population present, except in the most fortuitous cases. Therefore, population distributions determined from such a REMPI spectrum should be considered as a lower bound to the true vibrational excitation.

Even if the internal energy measurements of the nascent CH_3 photofragments are low, it is difficult to imagine that the remaining 48% of energy (*ca.* 20 kcal/mol) will be partitioned into the vibrational modes of the methyl product to which we are experimentally blind. More likely is that a significant fraction of the remaining energy is deposited into the kinetic energy of the methyl fragments. Similar effects have been observed in the photodissociation of acetone at 193 nm (see below), where the methyl fragments carry away over 40% of the available energy in their translational degrees of freedom.[9c] Our experimental apparatus is not suitable for measuring the kinetic energy deposited in the methyl fragments by the photodissociation.

The most striking result of this photodissociation is the production of a vibrational-state population inversion in the nascent SO photofragments. This inversion has been observed previously, and in agreement with our results here, but this work extends the measurement to higher vibrational levels. Nevertheless, both measurements indicate an inverted nascent vibrational distribution, peaked at $v'' = 2$. The observed vibrational distribution allows us to rule out direct photodissociation, *i.e.*, where absorption of a photon leads directly to a repulsive state, since the SO bond length in DMSO (1.49 Å)[23] is almost identical to that in diatomic sulfur monoxide (1.48 Å). A Franck–Condon analysis in the previous work was found to support a SO bond length of 1.55 Å in the sulfoxide immediately prior to dissociation. Either an excited electronic state of DMSO or CH_3SO was postulated to be the precursor to the vibrationally excited SO moiety. The data reported here also fits this argument well.

The measurements of the sulfur monoxide rotational state distributions indicate a relatively cold nascent radical that can be described by a temperature. The rotational temperatures are found to generally increase with increasing vibrational level, suggesting coupling between the rotational and vibrational motion in the transition state. We were not able to effectively measure the lower rotational levels ($N < 10$) due to spectral overlap, but simulations of these bands with the temperatures obtained from the higher levels give reasonable agreement. The observation of the SO radical appearing with a single temperature distribution

TABLE II: A Comparison of the Experimental and Calculated Relative Energy Distributions into the Fragments Following 193-nm Photodissociation of Acetone vs Dimethyl Sulfoxide[d]

		$(CH_3)_2CO$		$(CH_3)_2SO$	
fragment	deg of freedom	experiment[a]	model[b]	experiment[c]	model[b]
$CH_3(1)$	E_{int}	0.050	0.050	0.047	0.070
	E_{trans}	0.199	0.199	n.m.	0.291
CO, SO	E_{int}	0.172	0.195	0.213	0.052
	E_{tran}	0.163	0.190	0.211	0.157
$CH_3(2)$	E_{int}	0.050	0.068	0.047	0.081
	E_{trans}	0.199	0.299	n.m.	0.349
total		0.833	1.000	0.518	1.000

[a] Reference 9c. [b] Adapted from ref 24. [c] This work. [d] Relative energies are obtained with respect to the total available energy for the photofragments. The calculated values are obtained from an impulsive model and assume a stepwise cleavage of the bonds.

is consistent with the existence of only a single pathway to produce ground-state SO, *i.e.*, reaction 6 does not play a significant role.

We have thus far provided evidence that irradiation of DMSO at 193 nm proceeds along a single pathway to produce three fragments, two methyl radicals, and ground-state SO. But the question remains, does the three-body fragmentation occur by a concerted or stepwise mechanism? In this case, the lack of evidence for two different types of methyl, along with the inverted vibrational distribution, supports a concerted three-body fragmentation. The following scheme may be postulated: Absorption of a 193-nm photon by DMSO to give an excited state with a lengthened SO bond, which subsequently predissociates according to reaction 5.

To test this hypothesis, more data about the far UV spectroscopy of alkyl sulfoxides is necessary. Irradiation of DMSO at 193 nm is believed to be connected to a π–π^* type transition localized on the S–O chromophore. If this were the case, the excited state of DMSO would be expected to have a longer S–O bond length. Care must be exercised in assigning such localized bonding schemes in sulfoxides, because the d-orbitals of the sulfur atom can participate in forming the molecular orbitals, resulting in considerable electron delocalization.[7]

The similarities of the product state distributions from $(CH_3)_2SO$ and $(CH_3)_2CO$ seems to indicate that they may be dissociating by a similar mechanism. However, upon close examination of the product state distributions, small differences are indicative of the intermediate case (acetone) vs concerted (DMSO) dissociations (see Table II). If the diatomic fragments from acetone and DMSO and from CO and SO, respectively, are compared, small differences between the two cases exist. The CO fragment is produced with about one-half the vibrational energy and five times more rotational energy than the SO fragment. This can be understood in the following way. The greater vibrational energy content (and the inversion) of the SO photofragment are the result of a fast predissociative process dominated by the Franck–Condon excitation in DMSO, while in acetone the dissociation, comparable with that of a rotational period, allows more time to thermalize the energy into the other polyatomic fragments. The methyl rotational and v_2 vibrational distributions observed for DMSO both are slightly colder than those measured for acetone. Although some excitation was observed in the C–H stretch mode of methyl in the acetone dissociation, we see slightly more population in the case of methyl produced from DMSO.

The discrepancy between the two systems can be seen more clearly if one models DMSO in the stepwise dissociation limit. A simple extension of the impulsive model of Busch and Wilson[24] has been applied to the photodissociation of acetone and reasonably reproduces the experimental data, even if one considers the possible excess energy in the methyl fragments (see Table II). This classical model supposes that the dissociation occurs by a two-step mechanism and provides a rough estimate of the relative

energies in each fragment. If this model is applied to DMSO, it predicts *ca.* 15% of the available energy will be partitioned into the internal degrees of freedom of the methyl radicals and approximately 5% into rotation and vibration of sulfur monoxide. As can be seen in Table II, the model underestimates the amount of energy disposal into the SO photofragment and overestimates the amount of internal energy in the CH_3 radicals. This analysis suggests that this dynamical effect may result from the concerted three-body dissociation following irradiation of dimethyl sulfoxide at 193 nm.

Recent evidence suggests that three-body concerted dissociations are not all that rare. The 193-nm photodissociation of thionyl chloride (Cl_2SO) is a particularly compelling case, because of its structural similarities with DMSO. Baum *et al.* used photofragment time-of-flight spectroscopy to probe the 193- and 248-nm photodissociations of Cl_2SO. Their results indicate that following irradiation at 193 nm 80% of the photoexcited Cl_2SO dissociates by a concerted three-body mechanism to give SO + Cl + Cl. Wang *et al.* employed LIF spectroscopy to examine the quantum yield and energy disposal into the $SO(X^3\Sigma^-)$ fragment following 193- and 248-nm photolysis of Cl_2SO.[14] They concluded that 73% of the photoactivated Cl_2SO fragments via a concerted three-body dissociation to yield $SO(X^3\Sigma^-)$ following irradiation at 193 nm. Furthermore, the $SO(X^3\Sigma^-)$ produced from the 193-nm photolysis of Cl_2SO is born with an inverted vibrational distribution peaked at $v'' = 2$.

Summary and Conclusions

The quantum yield and vibrational and rotational population distributions of the nascent $SO(X^3\Sigma^-)$ radical from the photodissociation of $(CH_3)_2SO$ in the gas phase at 193 nm have been measured by laser-induced fluorescence, while the internal energy of the resulting neutral methyl fragments have been studied by REMPI spectroscopy. The energy distributions of the nascent fragments are best described by a concerted three-body fragmentation. While some of our data are suggestive of a concerted synchronous dissociation of the two S–C bonds in DMSO,[2] we cannot conclusively determine the synchronicity from our results. Further studies of the photofragment angular distributions following 193-nm irradiation of dimethyl sulfoxide would be helpful in analyzing this aspect of the dissociation dynamics.

Acknowledgment. We would like to acknowledge the generous support of this project by the Air Force Office of Scientific Research through Grants F49620-92-5-0406 and F49620-93-1-0110. Part of this research was carried out in the Puerto Rico Laser and Spectroscopy Facility, which operates under the auspices of the University of Puerto Rico and NSF-EPSCoR. H.H.N. and M.H. thank the Office of Naval Research for funding the work done at the Naval Research Laboratory.

References and Notes

(1) See, for example: *Molecular Photodissociation Dynamics*; Ashfold, M. N. R., Baggott, J. G., Eds.; Royal Society of Chemistry: London, 1987.
(2) Strauss, C. E. M.; Houston, P. L. *J. Phys. Chem.* **1990**, *94*, 8751.
(3) (a) Bock, H.; Solouki, B. *Angew. Chem., Int. Ed. Engl.* **1972**, *11*, 436. (b) Bock, H.; Solouki, B. *Chem. Ber.* **1974**, *107*, 2299.
(4) Plane, J. M. C. In *Biogenic Sulfur in the Environment*; Saltzman, E. S., Cooper, W. J., Eds.; ACS Symposium Series 393; American Chemical Society: Washington, DC, 1989; pp 404–23.
(5) Hudgens, J. W.; DiGiuseppe, T. G.; Lin, M. C. *J. Chem. Phys.* **1983**, *79*, 571.
(6) Chen, X.; Asmar, F.; Wang, H.; Weiner, B. R. *J. Phys. Chem.* **1991**, *95*, 6415.
(7) Gollnick, K.; Strauss, H. U. *Pure Appl. Chem.* **1973**, *33*, 217.
(8) (a) Gaines, G. A.; Donaldson, D. J.; Strickler, S. J.; Vaida, V. *J. Phys. Chem.* **1988**, *92*, 2762; (b) Donaldson, D. J.; Gaines, G. A.; Vaida, V. *J. Phys. Chem.* **1988**, *92*, 2766. (c) Hess, B.; Bruna, P. J.; Buenker, R. J.; Peyerimhoff, S. D. *Chem. Phys.* **1976**, *18*, 267; (d) Baba, M.; Shinohara, H.; Nishi, N. *Chem. Phys.* **1984**, *83*, 221.
(9) (a) Donaldson, D. J.; Leone, S. R. *J. Chem. Phys.* **1986**, *85*, 817. (b) Woodbridge, E. L.; Fletcher, T. R.; Leone, S. R. *J. Phys. Chem.* **1988**, *92*, 5387. (c) Trentleman, K. A.; Kable, S. H.; Moss, D. B.; Houston, P. L. *J. Chem. Phys.* **1989**, *91*, 7498. (d) Hall, G. E.; Vanden Bout, D.; Sears, T. J. *J. Chem. Phys.* **1991**, *94*, 4182. (e) North, S.; Longfellow, C.; Lee, Y. T., unpublished results.
(10) Felder, P.; Effenhauser, C. S.; Haas, B. M.; Huber, J. R. *Chem. Phys. Lett.* **1988**, *148*, 417 and references therein.
(11) Kawasaki, M.; Kasatani, K.; Sato, H.; Nishi, N.; Ohtoshi, H.; Tanaka, I. *Chem. Phys.* **1984**, *91*, 285.
(12) Kanamori, H.; Tiemann, E.; Hirota, E. *J. Chem. Phys.* **1988**, *89*, 621.
(13) Baum, G.; Effenhauser, C. S.; Felder, P.; Huber, J. R. *J. Phys. Chem.* **1992**, *96*, 756.
(14) Wang, H.; Chen, X.; Weiner, B. R. *J. Phys. Chem.*, preceding paper in this issue.
(15) Smith, W. H.; Liszt, H. S. *J. Quan. Spectros. Radiat. Trans.* **1975**, *11*, 45.
(16) (a) Ogorzalek-Loo, R.; Haerri, H. P.; Hall, G. E.; Houston, P. J. *J. Chem. Phys.* **1989**, *90*, 4222. (b) Moss, D. B.; Trentleman, K. A.; Houston, P. L. *J. Chem. Phys.* **1992**, *96*, 237.
(17) Barnhard, K. I.; Santiago, A.; He, M.; Asmar, F.; Weiner, B. R. *Chem. Phys. Lett.* **1991**, *178*, 150.
(18) Wiley, W. C.; McLaren, I. H. *Rev. Sci. Instr.* **1955**, *26*, 950.
(19) (a) Colin, R. *J. Chem. Soc., Faraday Trans. 2* **1982**, *78*, 1139; (b) Colin, R. *Can J. Phys.* **1969**, *47*, 979.
(20) Herzberg, G. *Molecular Spectra and Molecular Structure, I. Spectra of Diatomic Molecules*; R. E. Krieger Publishing Company: Malabar, FL, 1989.
(21) The following 193-nm absorption cross sections were used: SO_2 ($\sigma = 8.1 \times 10^{-18}$ cm^2 molecule^{-1}; from Okabe, H. *Photochemistry of Small Molecules*; Wiley-Interscience, New York, 1978; p 249) and $(CH_3)_2SO$ ($\sigma = 3.8 \times 10^{-18}$ cm^2 molecule^{-1}; from ref 7).
(22) Chen, X.; Wang, H.; Weiner, B. R., unpublished results.
(23) Dreizler, H.; Dendl, G. *Z. Naturforsch.* **1964**, *19A*, 512.
(24) Busch, G. E.; Wilson, K. R. *J. Chem. Phys.* **1972**, *56*, 3626, 3638.